- Technical Paper -

UTILIZING EXPANSIVE ADDITIVE TO REDUCE THERMAL CRACKING RISK OF RC SLAB ON SINGLE SPAN PC COMPOSITE GIRDER BRIDGE

Arifa I. ZERIN[*1], Akira HOSODA[*2], Satoshi KOMATSU[3] and Nobuyuki NAGATA[*4]

ABSTRACT

The highly durable concrete with blast furnace slag cement and expansive additive were utilized in the RC slab construction of Hikohei PC composite girder bridge. In the present research, FEM full scale structural model of Hikohei PC composite girder bridge has been successfully verified regarding early age thermal stress simulation. Simulated thermal stresses and consequent parametric studies have confirmed that thermal cracking risk is insignificant in PC composite girder RC slab with expansive additive when appropriate construction procedures are ensured avoiding extreme ambient conditions.

Key Words: Expansive Additive, Coefficient of Thermal Expansion, PC Composite Girder Bridge

1. INTRODUCTION

Hikohei post-tensioned segmented PC Composite Girder Bridge along Soma Fukushima Road in Fukushima prefecture built in July 2017 is the longest span (43.7 m) bridge of its kind. It consists of PC main girders, PC transverse mid-span and end-girders, PC slab as stay in place (SIP) forms and RC deck slab (Fig.1(a) and (b)). This structural system requires almost no form works facilitating rapid constructions. Previous investigations have revealed that RC decks constructed on simply supported PC girders and SIP forms exhibited less cracking risk than those constructed on continuous steel girders with removable forms [1], [2].

However, the RC bridge slabs in cold regions of Japan are susceptible to severe deterioration due to the combined effect of frost damage, chloride attack, ASR and fatigue caused by de-icing agent. Considering these severity, a multiple protection highly durable concrete with blast furnace slag (BBSG) cement, expansive additive, higher air content (5%), and low water-binder ratio (w/b=0.45) [3] were applied in Hikohei Bridge RC slab construction (Fig.1(c)) ensuring special construction and curing methods (Table1) [4]. Instrumented monitoring was performed by installing embedded strain gauges and thermocouples in RC deck slab to measure volumetric changes and temperature history of concrete (Fig.2(a)). Eventually, early age thermal and shrinkage cracks were effectively suppressed in Hikohei Bridge RC deck slab.

In the previous study [4] the early age volume changes of Hikohei Bridge slab were accurately simulated utilizing 3D FEM model successfully verified in real structural level. However, the previously established Hikohei Bridge FEM model [4] was based on the JSCE Standard Specifications for Design of
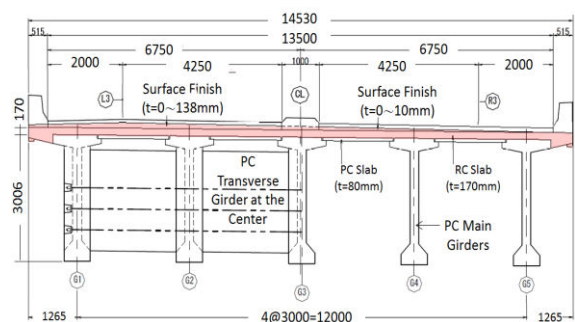

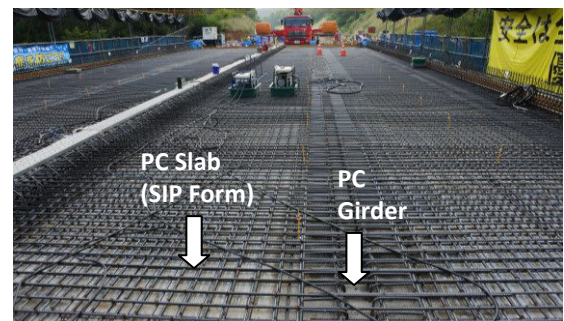Fig. 1(a) Cross-section of Hikohei Bridge (unit: mm)

Fig. 1(b) Construction of Hikohei Bridge

Fig. 1(c) Placing of highly durable concrete

Concrete Structures (2007) [5] regarding time dependent compressive strength, tensile strength and

*1   Post-Doctoral Researcher, Faculty of Urban Innovation, Yokohama National University, JCI Member
*2   Professor, Faculty of Urban Innovation, Yokohama National University, JCI Member
*3   Assistant Professor, Faculty of Urban Innovation, Yokohama National University, JCI Member
*4   IHI Construction Service Co., Ltd.

Table 1 Concrete mix proportion for Hikohei Bridge slab and test specimens

Concrete Mix	W/B %	s/a %	Air %	Slump	Unit Weight (kg/m³)						
					W	C	Ex	S1	S2	G1	AE+Ad
Design Value	45	44.4	5.0±1.5	12±1.5	173	365	20	382	376	410	3.85
BB[*]	45	44.4	5.9	10.5	172	385	-	382	376	410	3.85
BBEX[**]	45	44.4	6.7	11.0	173	365	20	382	376	410	3.85

[*]BBSG cement concrete without expansive additive, [**]BBSG cement concrete with expansive additive

Young's modulus development and reduction factors for Young's modulus development to consider the creep effect of concrete where the temperature adjusted effective material age of concrete [6] was not incorporated in the structural stress simulation.

In this context, the objective of the present study is the quantitative evaluation of the effectiveness of expansive additive in reducing the risk of thermal cracking in extreme conditions considering the influences of several parameters such as coefficient of thermal expansion (CTE), autogenous shrinkage, ambient temperature and initial concrete temperature on the generation of early age thermal and volumetric stress in RC slab. In order to achieve the target, extensive parametric studies were conducted utilizing the verified 3D FEM full-scale model for Hikohei Bridge incorporating temperature adjusted age of concrete which considers the effect of temperature history of concrete on time dependent strength and Young's modulus development based on the Guidelines of Control of Cracking of Mass Concrete 2016 [6].

2. VERIFICATION OF 3D FEM HIKOHEI BRIDGE MODEL BASED ON JCI2016 GUIDELINES

2.1 Structural Model of Hikohei Bridge

JCMAC3, the commercial finite element software designed for thermal and structural stress analysis of concrete structures incorporating JCI Guidelines for Control of Cracking of Mass Concrete (2016) has been utilized for consecutive thermal and structural stress analysis of 3D FEM full-scale Hikohei Bridge model. 3D linear hexahedral isoparametric heat generating and non-heat generating solid elements were applied for material models whereas 2D heat elements were modeled as heat transfer surfaces of 3D solid materials as heat transfer boundaries. Additionally, reinforcing bars were modeled with 1D truss elements in longitudinal and transverse directions of RC slab. Symmetric structural boundary conditions were applied on the Hikohei Bridge 1/4th FEM model (Fig.2(b)) [4]. Heat transfer coefficients for different heat transfer surfaces of the bridge were determined from parametric studies in thermal analysis considering real curing conditions and exposure of the surfaces as represented in Fig 2(b).

Fig.2(a) Locations of embeded strain gauges

Fig. 2(b) Hikohei bridge FEM model [4]

2.2 Material Models and Inputs

Fundamental material properties such as time dependent compressive strength and Young's modulus development, free autogenous shrinkage and setting time of multiple protection highly durable concrete (Table 1) for Hikohei RC slab were evaluated by laboratory investigations and utilized to calibrate input material models based on JCI Guidelines for Control of Cracking of Mass Concrete (2016) [6] incorporating the effective material age of concrete (Eq.1) considering the temperature history of the material as below

$$t_e = \sum_{i=1}^{n}\left\{\Delta t_i \cdot \exp\left[13.65 - \frac{4000}{273 + T(\Delta t_i)/T_0}\right]\right\} \quad (1)$$

where, t_e: effective material age (day) considering the effect of temperature history, Δt_i: period of constant temperature continuing in concrete (day), $T(\Delta t_i)$: concrete temperature for Δt_i (°C), T_o: value that makes temperature non-dimensional (1°C).

(1) Temperature Analysis Inputs

In temperature analysis module, the ambient temperature history monitored at Hikohei Bridge site (Fig.3(a)) was given as input. Monitored initial
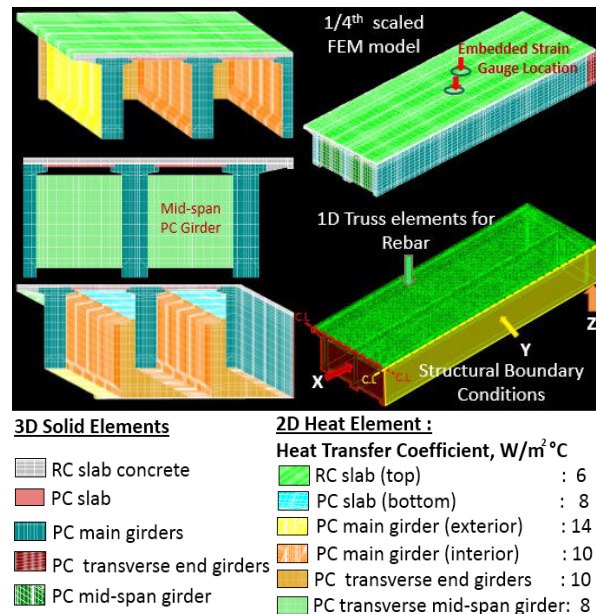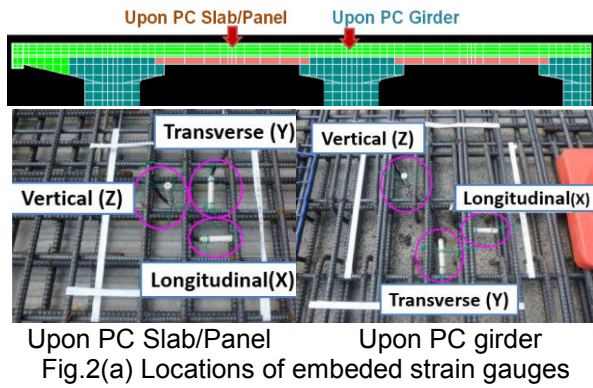
Table 2 Input material properties for temperature and stress analysis of Hikohei Bridge model

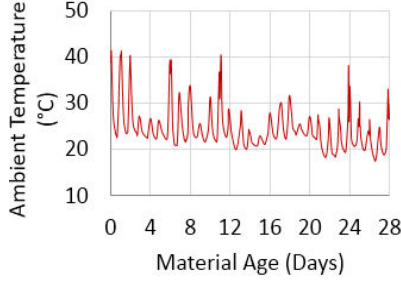| Properties	Deck Slab Concrete	Steel Bar	PC Girders	PC Slab
Heat Conductivity (W/m°C)	2.7	43	1.4	1.4
Specific Heat (kJ/kg°C)	1.15	0.47	1.15	1.15
Density (kg/m^3)	2300	7890	2300	2300
Young's Modulus (N/mm^2)	Calibrated JCI2016	2x10^5	36600	36600
Poisson's Ratio	0.2	0.3	0.2	0.3
Coefficient of Thermal Expansion (x10^{-6}/°C)	9.3	10	10	10

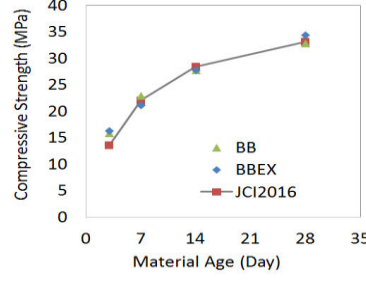Fig. 3(a) Recorded ambient temperature at Hikohei bridge site

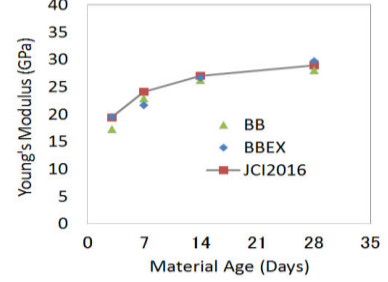Fig. 3(b) Compressive strength development
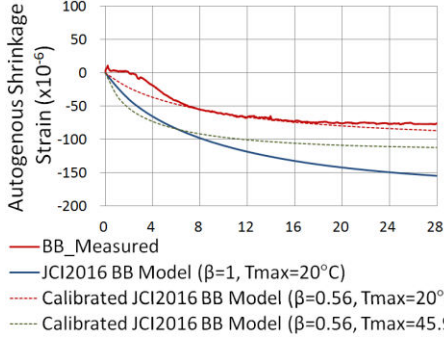

Fig. 3(c) Young's modulus development

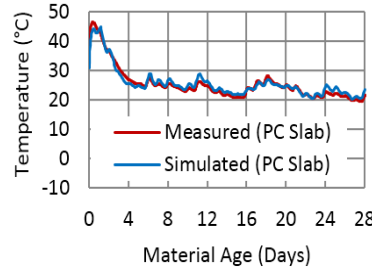Fig. 4(a) Calibration of autogenous Shrinkage model

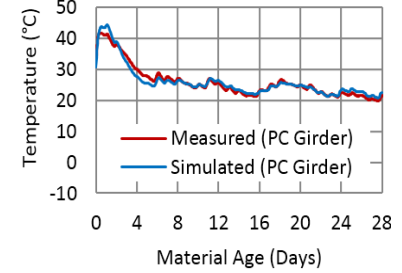Fig. 4(b) Simulation of concrete temperature upon PC slab

Fig. 4(c) Simulation of concrete temperature upon PC girder

placement temperature of slab concrete was 30.7°C whereas that of PC girders, PC slab and reinforcing bars is assumed as 31°C same as ambient temperature at the time of concrete placement of RC slab. Calibrated JCI2016 time dependent adiabatic temperature rise model (Eq.2) [6] was adopted in temperature analysis.

$$Q(t)=Q_\infty\left[1-exp\left\{-r_{AT}\left(t-t_{0,Q}\right)^{s_{AT}}\right\}\right] \quad (2)$$

where, $Q(t)$: adiabatic temperature rise at age of t days (°C), $Q_\infty(t)$: ultimate adiabatic temperature rise (°C) as a function of unit cement content and initial concrete placement temperature, r_{AT} and s_{AT}: parameters representing the rate of adiabatic temperature rise as functions of initial concrete placement temperature and $t_{0,Q}$: age of starting of adiabatic temperature rise. Other thermal properties such as heat conductivity, specific heat and density of slab concrete and adjacent materials are summarized in Table 2.

(2) Stress Analysis Inputs
Strength Development Models

JCI2016 equations for time dependent compressive strength and Young's modulus development of concrete (Eq.3 and Eq.4) were calibrated utilizing the laboratory investigation of BB

and BBEX concrete (Fig.3(b) and (c)). Moreover, JCI2016 time dependent equation of tensile strength development [6] has been adopted in the stress analysis (Eq.5).

$$f_c'(t_e)=\frac{t_e-S_f}{a+b\cdot\left(t_e-S_f\right)}f_c'(t_n) \quad (3)$$

$$E_c(t_e)=C_3\times f_c'(t_e)^{C_4} \quad (4)$$

$$f_t(t_e)=C_1\times f_c'(t_e)^{C_2} \quad (5)$$

where, t_e: effective material age (day), t_n: strength control age of concrete cured under water at 20°C (day): 28 days, $f_c'(t_e)$: compressive strength of concrete at t_e (N/mm^2), a=3.8 and b=0.7 are the calibrated parameters representing strength development, S_f : temperature adjusted age corresponding to initiation of hardening (day), $f_c'(t_n)$: compressive strength of concrete at t_n (N/mm^2). Further, $E_c(t_e)$: Young's modulus of concrete at t_e (N/mm^2) and calibrated parameters C_3=6000 and C_4=0.45. Moreover, $f_t(t_e)$: splitting tensile strength of concrete at t_e (N/mm^2) and parameters C_1=0.13 and C_2=0.85.

Effective Young's Modulus Considering Creep

Effective Young's modulus of concrete was adopted in the analysis introducing reduction factors at the age of temperature increasing and decreasing period

of concrete to include the effect of early age creep as recommended in JCI2016 in Eq.6 [6].

$$E_e(t_e) = \varphi(t_e) \times E_c(t_e) \qquad (6)$$

where, $E_e(t_e)$: effective Young's modulus at t_e (N/mm^2), $\varphi(t_e)$: Reduction factor, $\varphi(t_{max})$=0.42 until the effective material age of maximum temperature and $\varphi(t_{max+1})$=0.65 after one day of the effective material age of maximum temperature. $\varphi(t_e)$ is linearly interpolated between these two effective material ages.

Autogenous Shrinkage Model

The free maximum autogenous shrinkage obtained from laboratory investigation of BB concrete at 20ºC constant curing temperature was around 76x10^{-6} (Fig.4(a)) [4]. However, JCI2016 autogenous shrinkage equation (Eq.7) [6] for blast furnace slag cement incorporating the effect of maximum temperature of concrete produces autogenous shrinkage around 150x10^{-6} (JCI2016 BB Model (β=1, T_{max}=20°C) as shown in Fig.4(a)).

$$\varepsilon_{ag} = -\beta\varepsilon'_{as\infty} \times (1 - exp\ (-a \times (t'-t_s)^b)) \qquad (7)$$
$$\varepsilon'_{as\infty} = 2350 \times exp\ (-5.8 \times (W/C)) + \varepsilon'_{asT}$$
$$\varepsilon'_{asT} = 80 \times (1 - exp\ (-1.2 \times 10^{-6} \times (T_{max}-20)^4))$$

where, β : coefficient indicates the influence of cement and admixture (β=1 for blast furnace slag cement), t': effective material age, t_s : initial setting time, $\varepsilon'_{as\infty}$: final value of autogenous shrinkage, a, b : coefficient expressing the progressive characteristics of autogenous shrinkage, W/C : water cement ratio, ε'_{asT}: autogenous shrinkage contributed by maximum temperature and T_{max}: maximum concrete temperature. JCI2016 autogenous shrinkage BB model (Eq.7) has been calibrated by setting β=0.56 to obtain the test value for further utilization in simulation of Hikohei Bridge (Fig.4(a)).

Expansion Strain Energy Model

Expansion strain model based on the total energy conservation hypothesis [7] was applied in the present study to simulate the expansion strain of concrete with expansive additive. The expansion strain energy is obtained from the Eq.8 as follows.

$$U(t_e) = U_\infty . (1 - exp\ (-a\ (t_e-t_o)^b) \qquad (8)$$

where, $U(t_e)$: total energy at effective concrete age t_e, U_∞: ultimate value of the total energy, a and b : coefficient indicating the influence of the type of cement on the progressive characteristics of total energy, t_o : effective material age at the beginning of expansion. The parameters have been fixed as U_∞=110x10^{-6}, t_o=0.3, a=1.5 and b=1 for Hikohei Bridge slab concrete conducting extensive parametric studies utilizing the measured three directional strains in real Hikohei Bridge slab.

(3) Starting Point of Measurement and Simulation

Strain measurement before hardening of concrete incorporates very large strains and comparatively smaller stresses due to its plastic nature. Considering this fact, the starting point of strain measurement of Hikohei RC slab was decided from the starting point of hardening that can be equivalent to the initial setting time of concrete. Initial setting time of Hikohei concrete (BBEX in Table 1) was 0.17 day according to both Proctor and N-type setting time tests [4]. In this context, starting time of strength development, autogenous shrinkage and expansion strain was considered from 0.17 day of material age of concrete (initial setting time) in the structural stress simulation of Hikohei Bridge model corresponding to the starting time of strain monitoring in the real Hikohei Bridge RC slab. Simulation for early age volume changes was continued until 28 days of material age (period of wet curing) before the initiation of drying shrinkage.

Moreover, the value of Young's modulus, Poisson's ratio and CTE of concrete as well as other component materials were given inputs in the stress analysis module as depicted in Table 2.

2.3 Verification of Temperature and Strains

Simulation of temperature history of RC slab concrete upon PC slab and PC girder showed satisfactorily good agreement with the corresponding measurements (Fig.4(b) and (c)). Moreover, simulation of longitudinal (X) and transverse (Y) strains exhibited satisfactory agreement with the corresponding RC slab concrete strains measured upon PC slab and PC girder (Fig.5(a) and (b)). However, in Fig.5(a) and (b), simulated vertical (Z) strains were slightly differed from that of measured strains possibly due to the limitation of 3D expansion strain model based on the mechanical energy conservation hypothesis under restrained condition [7]. Further, the Hikohei model has less vertical restraints upon PC girders in absence of vertical shear connectors protruded from PC girders which might have simulated larger autogenous shrinkage compared to the real condition in vertical axis. It can be inferred that the 3D FEM full-scale Hikohei Bridge model has been successfully validated in terms of temperature and strain histories of RC deck slab.

3. SIMULATION OF STRESSES AND CRACKING INDEX OF HIKOHEI BRIDGE RC SLAB

Fig.6(a) and (b) demonstrate the simulated stresses along longitudinal (X) and transverse (Y) axes of RC deck slab of Hikohei Bridge FEM model. The maximum tensile stress along the bridge axis is 0.5 N/mm^2 whereas, there is no tensile stress generated along the transverses direction of the bridge deck. The cracking risk of the RC slab can be evaluated by calculating minimum Cracking Index (CI) defined by the ratio of the tensile strength of concrete and the tensile stress generated in the corresponding concrete component. Crack occurs when CI $\leq$ 1. The calculated minimum CI of the Hikohei Bridge RC slab upon PC girder was 4.6 at 11th day of material age while the tensile strength was 2.3 N/mm^2 at the same material age. Hence, the simulated stresses and cracking index represent that the cracking risk of Hikohei Bridge RC
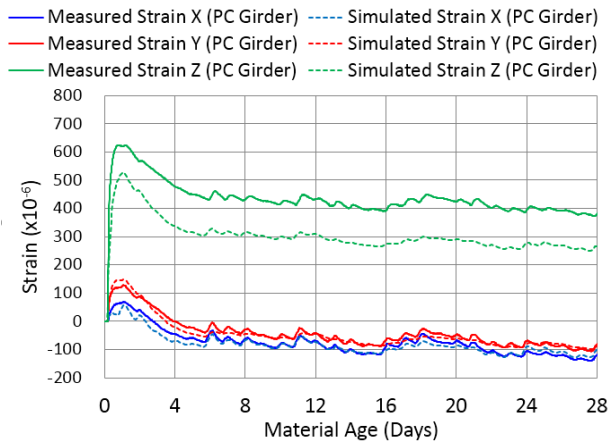
Fig. 5(a) Simulation of strains in RC slab upon PC girder along longitudinal (X), transverse(Y) and vertical(Z) axes
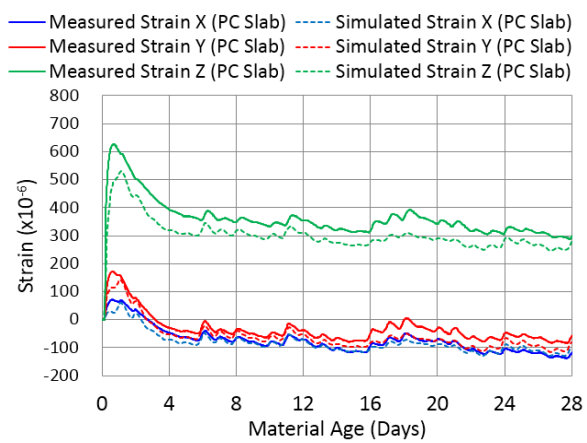
Fig. 5(b) Simulation of strains in RC slab upon PC slab along longitudinal(X), transverse(Y) and vertical(Z) axes
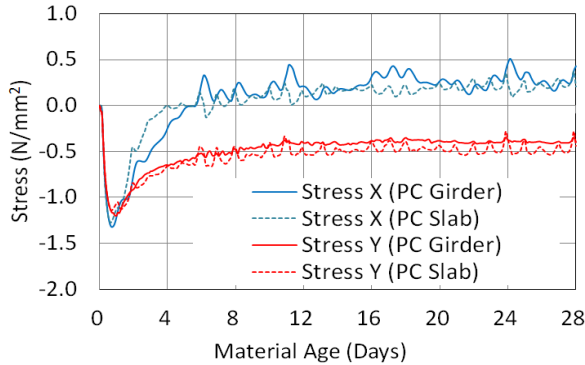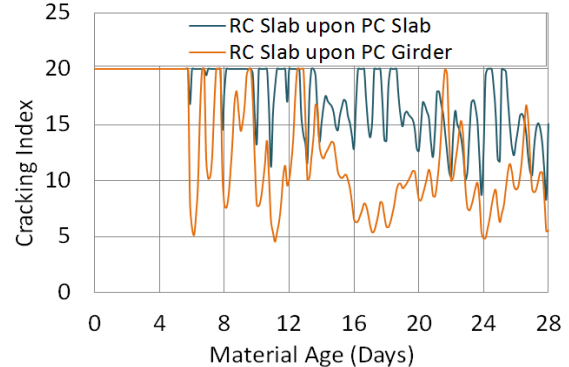

Fig. 6(a) Simulation of stresses in Hikohei RC slab

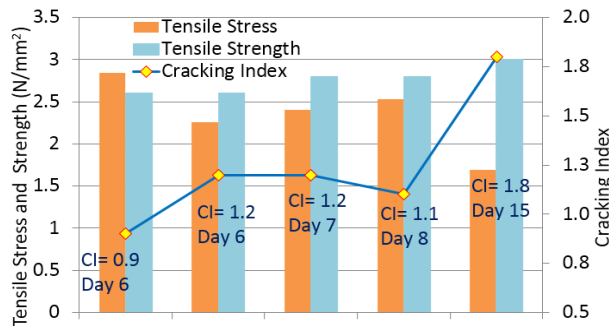Fig. 6(b) Cracking index of Hikohei RC slab

Case A: Ambient temperature=30°C, Initial concrete placing temperature=30°C, CTE=12x10⁻⁶/°C, JCI2016 autogenous shrinkage (β=1), No expansive additive

Case B: Calibrated JCI2016 autogenous shrinkage (β=0.56)
Case C: CTE=9x10⁻⁶/°C
Case D: Initial concrete placing temperature=20°C
Case E: Expansive additive is added

In case of B, C, D and E, other influential factors are same as demonstrated in case of A

Fig. 7 Effect of influential factors in reducing cracking index of RC slabs on PC composite girder bridges

slab is insignificant.

4. EVALUATION OF CRACKING RISK OF RC SLABS ON SINGLE SPAN PC COMPOSITE GIRDER BRIDGES

The validated 3D FEM Hikohei Bridge model has been further utilized to evaluate the cracking risk of RC slabs on single span PC composite girder bridges regarding several influential factors such as ambient temperature, initial concrete placing temperature, autogenous shrinkage, coefficient of thermal expansion (CTE) and chemical expansion of concrete on the basis of cracking index (CI). In Fig.7, the effects of these factors were evaluated by considering an extreme condition such as Case A without adding expansive additive, 30°C ambient and initial concrete placing temperature, JCI2016 autogenous shrinkage for blast furnace slag cement ((β=1) and large CTE=12x10⁻⁶/°C.

The minimum CI was appeared as 0.9 at material age of 6th day indicating that crack might occur in the RC slab concrete without expansive additive having large autogenous shrinkage and CTE placed in summer with high initial concrete temperature as the conditions considered in Case A. Alternatively in Case B, Case C and Case D, calibrated low autogenous shrinkage (β=0.56 in JCI2016 autogenous shrinkage equation Eq.7), comparatively lower CTE (9x10⁻⁶/°C) and low initial concrete temperature (20°C) were considered respectively. In those cases, cracking indices increased up to 20% to 30% reducing the risk of cracking. Nevertheless, in Case E, the minimum CI was increased by 100% owing to the addition of expansive additive minimizing the risk of cracking considerably even though larger CTE (12x10⁻⁶/°C) and autogenous shrinkage as well as higher ambient and initial concrete temperature were considered.

Table 3 Evaluation of cracking risk of RC slab of single span PC composite girder bridge

Ambient Temp (°C)	Initial Temp (°C)	Expansive Additive	CTE (x10⁻⁶/°C)	Material Age at Minimum CI	Tensile Strength at Minimum CI	Thermal Stress at Minimum CI	Cracking Index (CI)
30	35	X	12	6	2.59	3.17	0.8
		O	12	28	3.23	2.06	1.6
		O	9	28	3.23	1.40	2.3
	30	X	12	6	2.56	2.84	0.9
		O	12	14	2.99	1.68	1.8
		O	9	28	3.23	0.99	3.3
20	25	X	12	6	2.24	2.46	0.9
		O	12	28	3.08	1.60	1.9
		O	9	28	3.08	1.06	2.9
	20	X	12	7	2.32	2.30	1.0
		O	12	28	3.06	1.41	2.2
		O	9	28	3.06	0.94	3.3
10	15	X	12	28	2.84	2.72	1.0
		O	12	28	2.84	1.07	2.7
		O	9	28	2.84	0.61	4.6
	10	X	12	28	2.84	2.49	1.2
		O	12	28	2.84	0.90	3.2
		O	9	28	2.84	0.58	4.9

Moreover, extensive parametric studies were conducted to grasp the overall cracking risk of RC slabs of single span PC composite girder bridges in different ambient and initial temperatures, different CTEs, with and without expansive additives (Table 3). The parametric study results depicted in Table 3 have clearly identified that expansive additive is significantly effective in suppressing the risk of thermal cracking (minimum CI=1.6) in the corresponding RC slabs in a wide range of ambient temperatures from 10°C to 30°C whereas CTE is as large as $12x10^{-6}/°C$.

5. CONCLUSIONS

(1) Early age thermal stress simulation of verified FEM real structural model of PC composite girder bridge has revealed that the cracking risk of Hikohei Bridge RC slab incorporating blast furnace slag cement and expansive additive is insignificant due to the considerably low thermal stress generation.

(2) Parametric studies utilizing the established Hikohei Bridge FEM model have confirmed that thermal cracking risk is almost zero in RC slabs with expansive additives ensuring appropriate construction procedures on PC composite girder bridges except extremely severe ambient conditions.

ACKNOWLEDGEMENT

REFERENCES

[1] P. D. Cady, R. E. Carrier, T. A. Bakr and J. C. and Theisen, "Final Report on the Durability of Bridge Deck Concrete, Pennsylvania Department of Transportation," Harrisburg, PA, pp.153, 1971.

[2] L.J. Eppers, C.E. French and J.Hajjar, "Transverse Cracking in Bridge Decks: Field Study," Summary Report 1999-05, Minnesota Department of Transportation, St. Paul, MN, pp.103, 1998.

[3] T. Ishida and I. Iwaki, "Multi-scale and Multi-chemo-physical Modeling of Cementitious Composite and Its Application to Early Age Crack Assessment of Reinforced Concrete Slab Decks," in 2nd RILEM/COST Conference on Early Age Cracking and Serviceability.

[4] A.I. Zerin, A. Hosoda, S. Komatsu and N. Nagata, "Numerical simulation of thermal stress in highly durable RC slab on pc composite girder bridge," in JCI Annual Convention, Kobe, 2018.

[5] Japan Society of Civil Engineering, Standard Specifications for Design of Concrete Structures, JSCE, 2007.

[6] Japan Concrete Institute, JCI Guidelines for Control of Cracking of Mass Concrete, Tokyo, 2016.

[7] T. Tanabe and Y. Ishikawa, "Chemical Expansion Effect in Concrete and its Numerical Simulation Based on the Mechanical Energy Conservation Hypothesis," in JCI-RILEM International Workshop on Control of Mass Concrete and Related Issues Early Age Cracking of Structures (CONCRACK), Tokyo, 2017.